DOI: 10.1002/ejic.200600829

The Hydrothermal Synthesis of Transition Metal Complex Templated Octamolybdates

Katikaneani Pavani,[a] Samuel E. Lofland,[b] Kandalam V. Ramanujachary,[c] and Arunachalam Ramanan*[a]

Keywords: Solvothermal synthesis / Molybdenum / Supramolecular chemistry / Organic–inorganic hybrid composites

The hydrothermal reaction of an aqueous ammonium heptamolybdate solution with cobalt or copper metal salts in the presence of imidazole (imi) or pyrazole (pz) in the temperature range 120–180 °C and at autogenous pressure yields four fully oxidized metal-complex-templated octamolybdates, namely $[\{Cu^{I}(imi)_2\}_4(imi)_2Mo_8O_{26}]\cdot 4H_2O$ (**1**), $(Himi)_2[\{Cu^{II}(imi)_2\}_2Mo_8O_{27}]$ (**2**), $[\{Co^{II}(pz)_4\}_2(pz)_2Mo_8O_{26}]$ (**3**), and $[\{Cu^{II}(pz)_4\}_2Mo_8O_{26}]\cdot 2H_2O$ (**4**). The single-phase nature of the solids was established by single-crystal and powder X-ray diffraction, thermal analysis, and spectroscopic techniques. Compounds **1**, **3**, and **4** are neutral composite solids – **1** is a discrete molecular unit while **3** and **4** are 2D sheets. Compound **2** consists of anionic chains with imidazolium counter cations. The influence of the metal complex and temperature of the hydrothermal reaction on the formation of the different hybrid solids built of octamolybdate clusters is discussed. We also provide plausible mechanisms for the self-assembly of the crystals in terms of supramolecular organization between metal complexes and soluble molybdenum precursors in the initial stages of the reaction. The magnetic properties of **2**, **3**, and **4** confirm the presence of Cu and Co in the divalent state with no appreciable long-range order down to 5 K, whereas **1** is diamagnetic.

Introduction

Polyoxomolybdate (POM) cluster anions are ideal nanobuilding blocks to assemble giant molecular crystals exhibiting compositional variation and structural diversity.[1,2] A contemporary interest in this area is to employ organic components or metal complexes to dictate the formation of novel organic–inorganic hybrid composites as these show promising applications in the areas of catalysis, magnetism, photochemistry, sensors, and energy storage.[3–6] A large number of POM-based solids have been self-assembled from aqueous solution in the presence of organic molecules as structure directors.[7–9] In particular, the role of organic diamines in the formation of discrete POM clusters to three-dimensional networks of molybdenum oxide based materials has been investigated extensively.[10–12] It is well established that solids crystallized from aqueous molybdate solution under either ambient or hydrothermal conditions in the presence of organic diamines are predominantly based on organic–inorganic hybrid salts. These may be salts between organic ammonium cations and discrete POM anions or composite solids with extended POM anions incorporated with organic cations.[13,14] If an additional transition metal ion is present, the metal complex formed in situ can either occur as the counter cation or derivatise the POM anion, or they can also be part of the extended network linking POM cluster anions.[15–17] In selected cases, the organic ammonium ions can take part in unusual hydrogen bonding and/or π-π interactions, which, in turn, can direct the crystal packing.[18] In an attempt to rationalize the reactivity pattern in the formation of these solids under hydrothermal conditions, we have been systematically analyzing the chemistry involved in controlling the reaction and hence the structure of molybdates, even though hydrothermal reactions are commonly termed as "black box" in nature. Apart from pH, molybdenum's ability to coordinate with aromatic diamines to form either pillared or composite solids is also important.[19] Another issue is the nature of the complex formed between the organic amine and the transition metal ion and its stability under hydrothermal conditions. Frequently, some of these organic amines can reduce transition metals under hydrothermal conditions and hence can lead to a different metal complex in situ. In addition, the temperature of crystallization is important. Apart from these, nonbonding interactions taking place between molybdate cluster anions and organic groups along with water molecules will influence the crystal structure packing. In our earlier work,[20] we have shown how a weak

[a] Department of Chemistry, Indian Institute of Technology, New Delhi 110016, India
Fax: +91-11-2658-2277
E-mail: aramanan@chemistry.iitd.ac.in
[b] Department of Physics and Astronomy, Rowan University, Glassboro, New Jersey 08028, USA
[c] Department of Chemistry and Biochemistry, Rowan University, Glassboro, New Jersey 08028, USA

Supporting information for this article is available on the WWW under http://www.eurjic.org or from the author.

ligand such as 2-aminopyridine ($pK_a \approx 6.9$) affects the hydrolysis and condensation reactions taking place in aqueous molybdate solution containing first-row transition metal ions.

Acidification of aqueous molybdate solution in the presence of organic cations yields a variety of POM cluster anions with varying numbers of molybdenum atoms. Among them, the octamolybdate anion **A** (Figure 1, left) with the composition $[Mo_8O_{26}]$ is predominant.[21–23] This cluster anion exhibits different isomeric structures; the cluster can occur either as discrete entities (zero-dimensional) or act as building blocks for 1D chains, 2D sheets, or 3D frameworks.[24–26] Another octamolybdate cluster, **B**, which has a different composition $[Mo_8O_{28}]$ (Figure 1, right), is observed in a few solids although in only one example does it exist as a discrete cluster.[27] While Mo_8O_{26} is rarely protonated,[28,29] the cluster anion Mo_8O_{28} is possibly protonated in aqueous solution and hence has a strong tendency to become derivatized or condensed under suitable conditions.[30–32] In this paper, we explore the reaction conditions necessary to form the octamolybdate cluster anion as a versatile inorganic building block for the construction of new hybrid molybdates in the presence of imidazole and its isomer pyrazole as templates. We also discuss the formation of **1**–**4** in terms of ideas recently proposed by Ramanan and Whittingham[33] for the formation of metal organic polymers and later extended to explain the formation of copper coordination polymers based on molybdates crystallized under hydrothermal conditions.[34]

Results and Discussion

The hydrothermal reaction of copper and cobalt salts in the presence of imidazole (imi) or pyrazole (pz) at different temperatures leads to different products. Powder and single crystal XRD, TGA, and FTIR analysis were employed to establish the crystal structure, phase purity, and composition. Scheme 1 summarizes the optimal reaction conditions employed to obtain monophasic solids.

Crystal Structure of 1

The crystal structure of $[\{Cu^{I}(imi)_2\}_4(imi)_2Mo_8O_{26}]\cdot 4H_2O$ (**1**) shows the presence of a discrete octamolybdate cluster (type **B**) derivatized by two imidazole moieties and

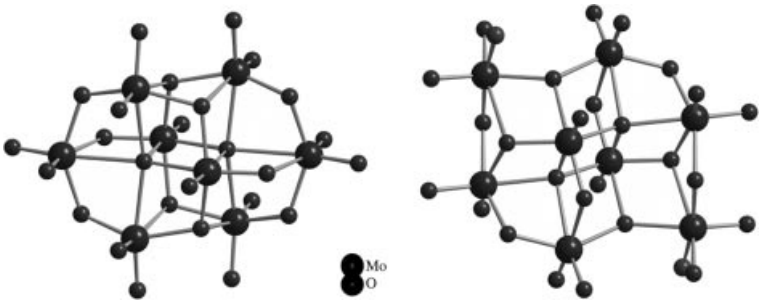

Figure 1. A view of (a) the β-octamolybdate anion $[Mo_8O_{26}]$ (type **A**) and (b) the octamolybdate anion $[Mo_8O_{28}]$ (type **B**).

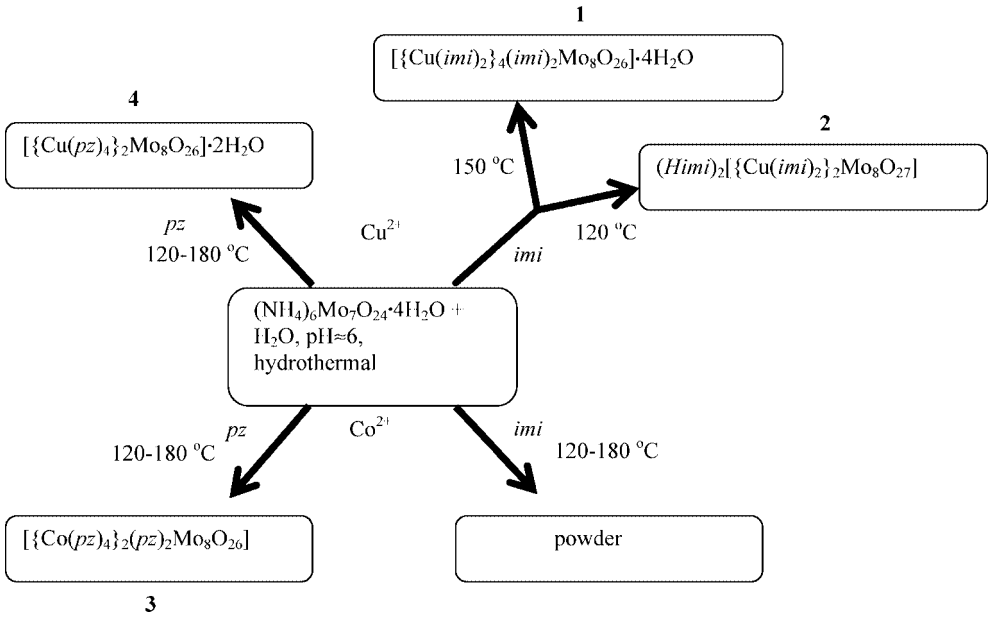

Scheme 1. Experimental details.

four tricoordinate copper imidazole complexes (Figure 2). An inversion center occurs in the center of the cluster anion. Each molybdenum atom in the $\{Mo_8O_{26}N_2\}^{4-}$ cluster anion has a distorted octahedral environment with six oxygen atoms. The thirteen asymmetric oxygen atoms in this cluster anion fall into four groups: seven are terminal, three are doubly bridging, two are triply bridging, and one is a quadruply bridging ligand. The copper(I) imidazole complex has two imidazole ligands and the third coordination is to the terminal oxygen of the cluster anion. In all the examples reported in the literature, derivatization of the cluster anion with an organic moiety (e.g. acetate or formate groups) appears to take place only on the molybdenum containing three terminal oxygens.[35,36] An interesting feature of this structure is that copper occurs in the +1 oxidation state and is tricoordinate. The supramolecular assemblies based on the derivatized octamolybdate unit $[\{Cu^{I}(imi)_2\}_4(imi)_2Mo_8O_{26}]$ are further connected to each other through strong H-bonding interactions of the type N–H···O (see Figure S1 in the Supporting Information). Apart from these, C–H···π interactions with an angle of 123.17° also dominate the crystal packing (Figure 3). Such copper(I) tricoordination is seen in the literature for β- and γ-octamolybdate cluster anions.[37–39] Complex **1** appears to be similar to one reported in the literature even though we have prepared it under different reaction conditions.[40]

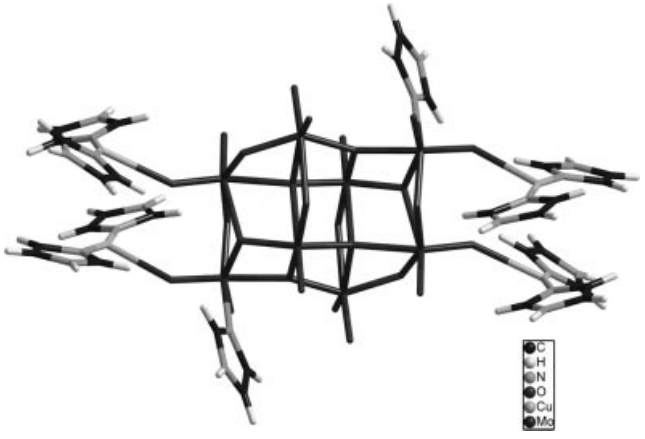

Figure 2. Crystal structure of the discrete octamolybdate **B** in **1** derivatized by two imidazole groups and four tricoordinate copper imidazole complexes.

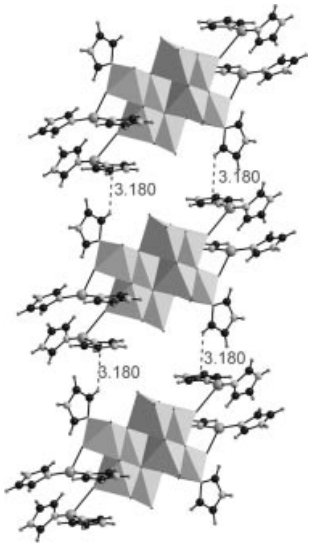

Figure 3. C–H···π interactions (Å, dotted lines) dominating the packing of the unit cell in **1**.

Crystal Structure of 2

The crystal structure of $(Himi)_2[\{Cu^{II}(imi)_2\}_2Mo_8O_{27}]$ (**2**) consists of imidazolium cations and infinite $\{Mo_8O_{27}\}_\infty$ chains connected to square-pyramidal copper complexes (Figure 4). The $\{Mo_8O_{27}\}_\infty$ chain propagates along the *a*-axis and is surrounded by six others (see Figure S2 in the Supporting Information). The inter-chain regions are filled with imidazolium cations that participate extensively in strong hydrogen bonding with the cluster oxygens. An interesting feature observed in the crystal structure is the strong π···π interaction between the imidazole groups coordinated to the copper atoms of two adjacent chains (Figure 5). The Mo–O distances are significantly different due to their multiple bonding character and range from 1.687(3) to 2.504

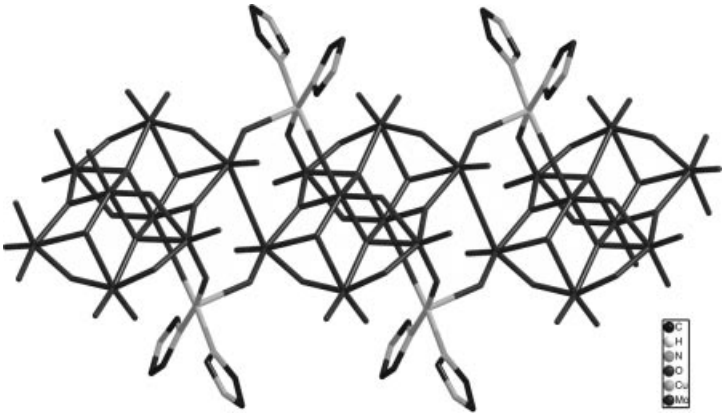

Figure 4. Anionic molybdenum oxide chains $\{Mo_8O_{27}\}^{6-}$ built from the octamolybdate clusters of type **B** sharing corners and also coordinated to square-pyramidal copper complexes in **2**.

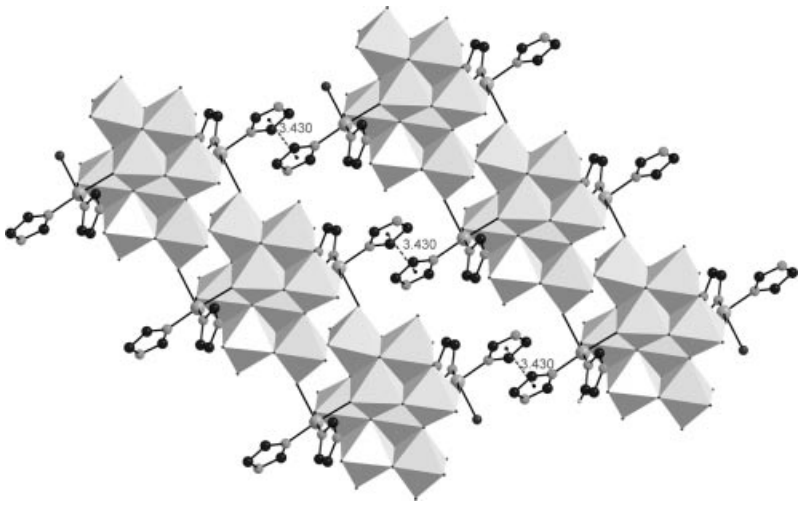

Figure 5. Strong π···π interactions (Å, dotted lines) between copper-coordinated imidazole groups of two adjacent chains in **2**.

(3) Å; the Cu–O distances range from 2.134 to 2.315 Å. A sixth Cu–O distance is 2.705 Å. The octamolybdate chains found in **2** are similar to those of $(NH_4)_6Mo_8O_{27}\cdot 4H_2O$[41] and $(C_4H_{12}N_2)_3Mo_8O_{27}$,[42] which are built from type **B** clusters, but with different counter cations such as ammonium or protonated amines. A similar metal coordination to the molybdate chain has been found previously in the case of rare-earth metals like samarium[43] and europium.[44] However, this is the first example of a transition metal organic complex coordinating with the chain. The structure is also special as the same organic group occurs as the counter cation as well as a coordinating unit during self-assembly.

Crystal Structure of 3

The single-crystal analysis of $[\{Co^{II}(pz)_4\}_2(pz)_2Mo_8O_{26}]$ (**3**) shows the presence of octamolybdate (type **B**) derivatized by two pyrazole moieties and covalently bonded to the four cobalt pyrazole square-planar complexes (see Figure S3 in the Supporting Information). Each cobalt complex in this structure is covalently linked to two octamolybdate cores by a singly bridging oxo ligand. The Co^{II} sites exhibit octahedral geometry $\{CoN_4O_2\}$ in such a way that each cobalt ion is coordinated to four nitrogen donors of pyrazole in the basal plane and two bridging oxo groups of the octamolybdate clusters at the apical position, thereby forming the 2D network shown in Figure 6. Linkage of cobalt complexes through molybdate clusters has rarely been reported in the literature, and this is the first example where a cobalt complex is covalently linking the derivatized octamolybdate. There are two other examples where cobalt complexes are linked to the β-octamolybdate cluster anion $[Mo_8O_{26}]$ (type **A** in Figure 1a).[24] This structure is a unique example where the derivatized $[Mo_8O_{28}]^{[8]-}$ is covalently linked to metal complexes to extend it into a 2D network.

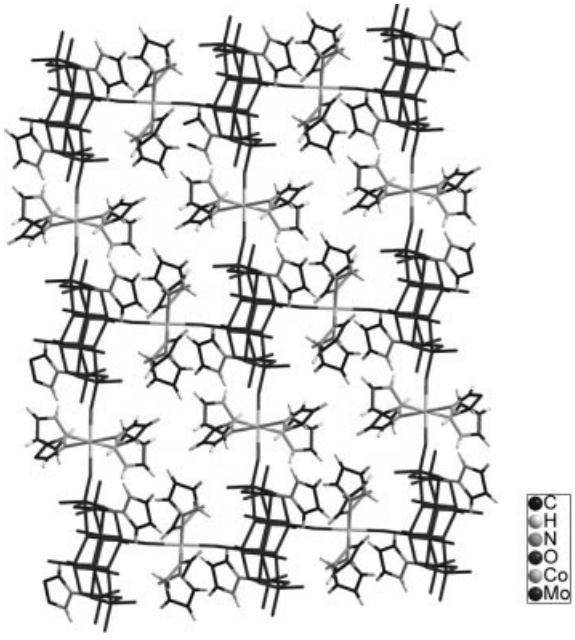

Figure 6. Pyrazole-derivatized octamolybdate cluster **B** linked through square-planar cobalt pyrazole complexes forming 2D sheets in **3**.

Crystal Structure of 4

Solid $[\{Cu^{II}(pz)_4\}_2Mo_8O_{26}]\cdot 2H_2O$ (**4**) contains β-octamolybdate clusters (type **A**) that are covalently linked to four square-planar $\{Cu(pz)_4\}^{2+}$ complexes to form 2D sheets with isolated water molecules (Figure 7). The $\{Mo_8O_{26}\}^{4-}$ cluster unit is identical to the well-documented β form, with eight edge-sharing MoO_6 octahedra where all molybdenum atoms are in the +6 oxidation state. Each copper complex in this structure is covalently linked to two octamolybdate cores by a singly bridging oxo ligand (see Figure S4 in the Supporting Information). The Cu^{II} sites exhibit an octahedral geometry $\{CuN_4O_2\}$ such that each copper center is

coordinated to four nitrogen donors of pyrazole in the basal plane and two bridging oxo groups of the octamolybdate clusters at the apical positions, thus extending it into a 2D network. A number of structures where octamolybdate clusters are covalently bonded to $\{M(ligand)\}^{n+}$ complexes have been described previously,[24–26] although the framework in **4** is unique. There are a few other solids based on β-octamolybdate clusters covalently linked through copper. In $[\{Cu(2,2'\text{-bipy})_2\}_2Mo_8O_{26}]$,[45] the β-octamolybdate cluster is linked to two square-pyramidal copper bipyridyl complexes and occurs as a supramolecular entity. In $[\{Cu_2(C_8H_6N_2)_2(C_7H_6N_2)\}_2Mo_8O_{26}]$,[46] the copper complex with two bidentate ligands links β-octamolybdate clusters into 1D chains. On the other hand, in $[\{Cu(o\text{-phen})_2\}_2Mo_8O_{26}]$ and $[\{Cu(en)_2\}_2Mo_8O_{26}]$, octamolybdate clusters are reported to adopt the α and γ forms, respectively.[47]

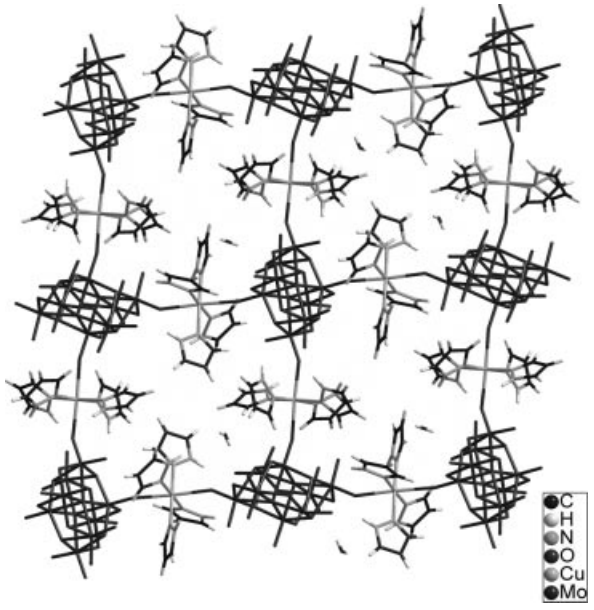

Figure 7. The 2D network observed in **4** involving the linkage of the octamolybdate anion $[Mo_8O_{26}]$ (type **A**) to square-planar copper pyrazole complexes.

Chemistry of Formation of Hybrid Solids Based on Octamolybdate Anions

The cobalt or copper salts and the amines used as templates in this work were employed under identical reaction conditions (in terms of molybdate precursor, concentration, volume of the solution, molar ratios of the reacting species) to examine the nature of the molybdates formed. The selected amines act as good complexing agents and are stable under hydrothermal conditions. In addition, they have similar pK_b values and therefore do not affect the pH of the reaction medium considerably. We also varied the tempera-

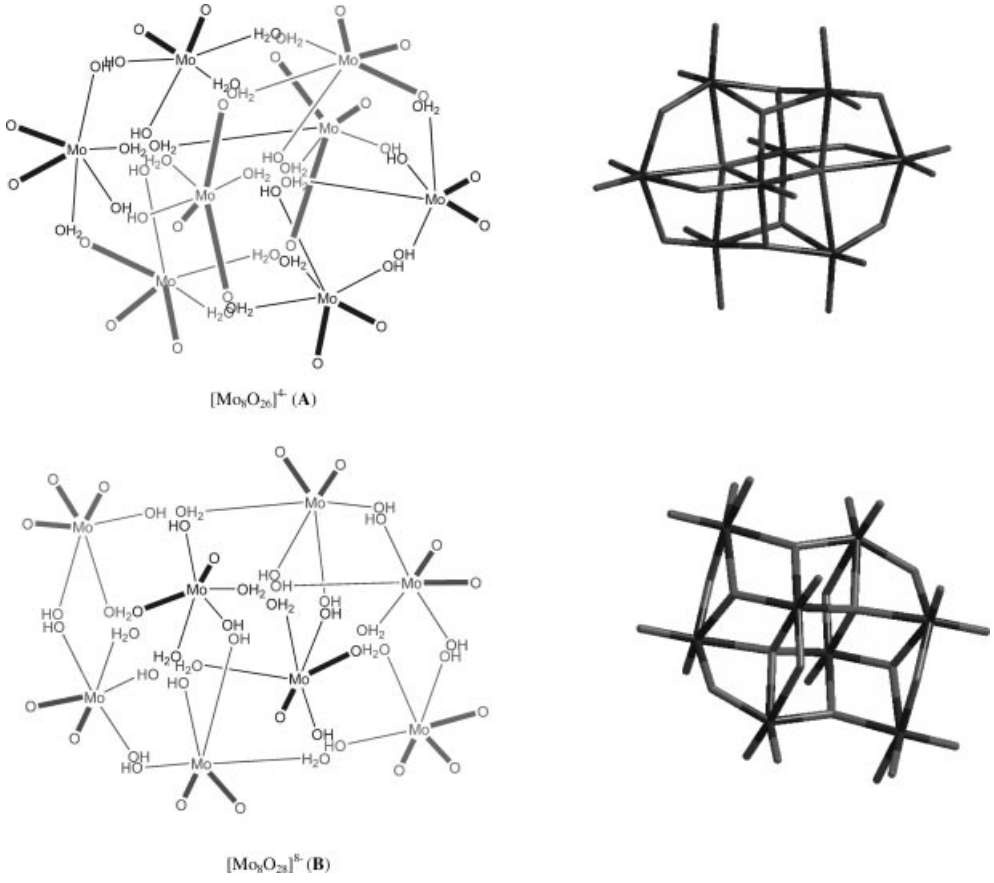

Scheme 2. A hypothetical scheme for the self-assembly of octamolybdate cluster anions **A** and **B** from the condensation of neutral molybdenum precursors.

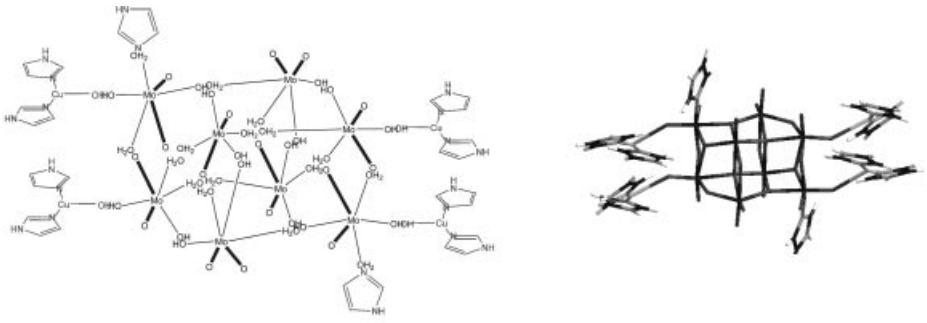

Molecular assembly leading to discrete neutral clusters based on **B** in $[\{Cu(imi)_2\}_4(imi)_2Mo_8O_{26}]\cdot 4H_2O$, **1**

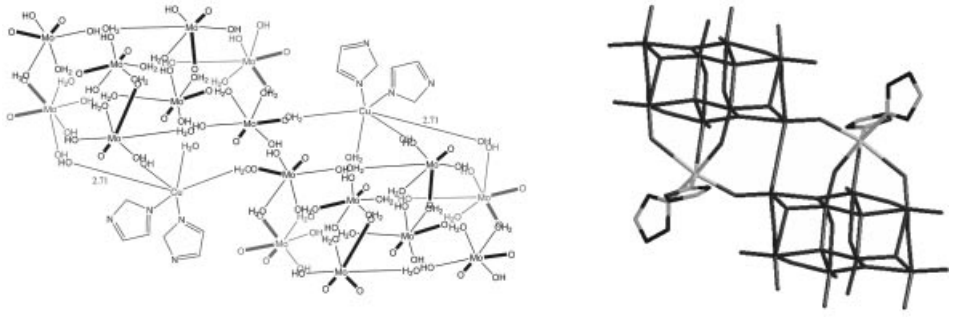

Molecular assembly leading to anionic 1D chains in $[\{Cu(imi)_2\}_2Mo_8O_{27}]^{2-}$, **2.** The counter cations (*Himi*) are not shown.

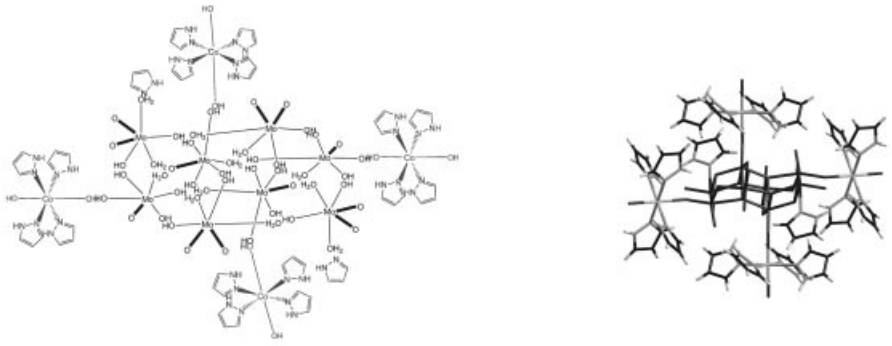

Molecular assembly leading to neutral 2D sheets based on **B** in $[\{Co(pz)_4\}_2(pz)_2Mo_8O_{26}]$. **3**

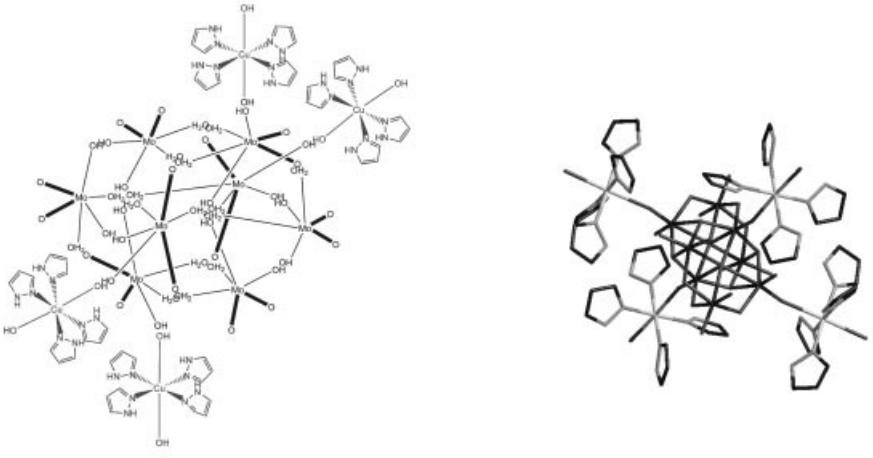

Molecular assembly leading to neutral 2D sheets based on **A** in $[\{Cu(pz)_4\}_2Mo_8O_{26}].2H_2O$, **4**

Scheme 3. A hypothetical scheme for the self-assembly of compounds **1**–**4** from the molecular precursors.

ture (and indirectly the autogenous pressure) to understand its effect on the nature of the products formed. When the heptamolybdate cluster anion is dissolved in aqueous solution in the presence of an organic diamine (pz or imi) and a cobalt or copper salt, a number of cluster anions, including $[Mo_8O_{26}]^{4-}$ (**A**) or $[H_xMo_8O_{28}]^{-(8-x)}$ (**B**), self-assemble due to hydrolysis and condensation of neutral and/or anionic molybdenum precursors, the assembly of which depends on the pH, ionic strength, and polarity of the medium. An examination of the literature shows that **A** is the dominant cluster found in several solids crystallized from acidified aqueous molybdate solution. However, in the majority of these solids **A** occurs as a discrete unit, whereas **B** occurs as a discrete protonated cluster in only one example[27] as it invariably gets derivatized by the organic group or condensed to form a 1D chain through three kinds of linkages, i.e. sharing edges, corners and pair –M–O–M– bridges,[20] or links through metal complexes to form 2D sheets (see Figure S5 in the Supporting Information). This is probably due to the large negative charge present on the anion **B**. Crystallization of **1**–**3** as well our previous report suggests that cluster **B** can also act as a building block to form multidimensional structures under favorable conditions. One can interpret the formation of **1**–**3** based on the complexing strength of the ligand and their lability with hydroxy groups in aqueous solution. In our earlier work, we also observed that in the presence of a better leaving group, such as 2-aminopyridine, cobalt yielded a heptamolybdate while copper yielded Lindgrenite-type copper molybdate as both cobalt and copper complex weakly with 2-aminopyridine.[20] In the presence of imi, copper forms a bis complex by *cis* addition. This prefers to derivatize cluster **B** and form the supramolecular assembly in **1** (Figure 2). In contrast, the reaction in the presence of pz leads to the formation of the square-planar complex $\{Cu(pz)_4\}^{2+}$, which crystallizes with the counter anion **A** to yield the solid **4**. On the other hand, the reaction of imi with cobalt yields only a powder that could not be structurally characterized. Reaction of cobalt with pz forms the complex $\{Co(pz)_4\}^{2+}$, which coordinates with **B** and crystallizes as **3**. We also note that the heteroatom of the organic moiety plays two roles: it provides a coordination linkage and acts as a charge compensator if necessary. The temperature does not affect the product if the metal complexes formed are stable in the presence of the organic amine (**3** and **4**). Imidazole is a better reducing agent than pyrazole, and hence $[Cu(H_2O)_4(imi)_2]^{2+}$ is readily reduced at higher temperature to form $[Cu(H_2O)(imi)_2]^{+}$, which derivatises **B** to form **1**.

Ramanan and Whittingham[33] have recently postulated a hypothetical mechanism for the formation of metal organic polymers from soluble molecular species. Pavani et al. have extended this approach to rationalize the formation of cop-

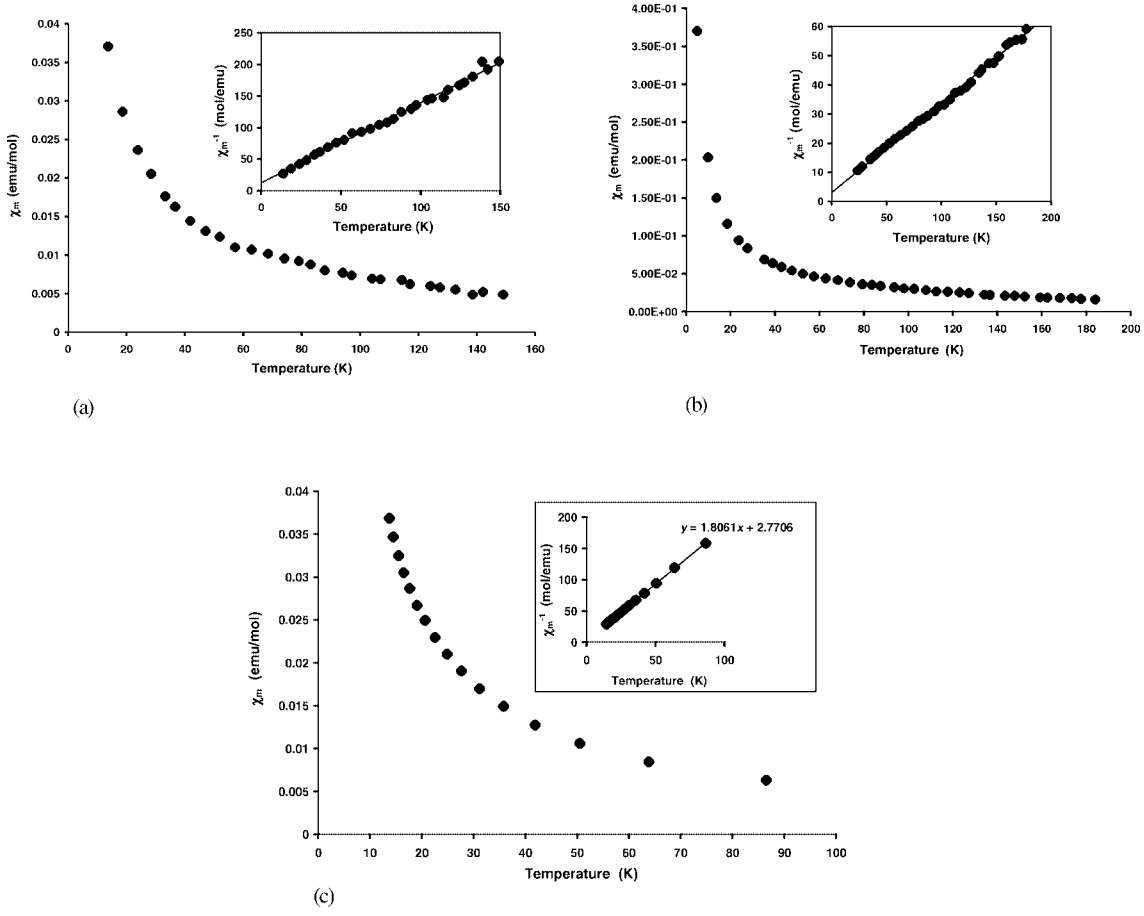

Figure 8. χ_m and χ_m^{-1} (insets) vs. *T* plots for (a) **2**, (b) **3**, and (c) **4**.

per coordination polymers based on molybdates under hydrothermal conditions.[34] Here, we have employed a similar strategy to understand the self-assembly of octamolybdate complexes that incorporate a copper/cobalt amine complex and/or the amine. Scheme 2 shows the proposed formation of the two cluster anions **A** and **B** from the condensation (dehydration) of monomeric molybdenum precursors. While **A** is built from two precursors, one neutral and another anionic, **B** forms from three types of molybdenum precursors. The formation of hybrid salts based on **A** can be visualized in terms of supramolecular aggregation of ion pairs formed between a molybdenum anionic precursor and organic cation along with a neutral molybdenum precursor. The presence of a large negative charge on **B** makes it unstable and the supramolecular aggregation is redefined to yield extended molybdate chains through edge-shared, pairs of vertex-shared, or vertex-shared clusters with K, NH_4, 2-ampy, picolinium, hexylammonium, etc. cations (as shown in Scheme S1 in the Supporting Information). However, when the solutions contain metal amine complexes and uncomplexed amines different supramolecular assemblies occur. In Scheme 3 we have proposed a plausible model to account for the formation of **1**–**4**.

Magnetic Properties

The presence of $Cu^{II}(d^9)$ in **2**, **4** and $Cu^{II}(d^7)$ in **3** prompted us to carry out a magnetic study of these materials. The vast structural diversity of polyoxomolybdates and their ability to incorporate a large number of 3d metal cations opens synthetic routes to new magnetic molecules in which a diamagnetic molybdate framework acts as an efficient mediator of magnetic superexchange. The thermal variations of χ_m and χ_m^{-1} in the temperature range 5–160 K for **2**, **3**, and **4** are shown in Figure 8. The molar magnetic susceptibility was corrected for the diamagnetic corrections of the core electrons of the ions and functional groups. The linear portions of the plots were fitted to the Curie–Weiss relation given below, where θ is the Weiss constant and C is the Curie constant. The Weiss constants are –10, –10, and –1.5 K for **2**, **3**, and **4** respectively.

$$\chi_m = C/(T - \theta)$$

The negative values of the Weiss constant indicate that the precursor exchange interactions are dominantly antiferromagnetic, although no long-range ordering was observed down to 5 K in these samples. As already mentioned, the structures consist of copper complexes that are well separated by the diamagnetic octamolybdate cluster units $\{Mo_8O_{28}\}^{8-}$ and $\{Mo_8O_{26}\}^{4-}$. The exchange correlations can be attributed to the superexchange couplings between the copper(II) or cobalt(II) ions. The effective magnetic moments calculated for **2**, **3**, and **4** are 2.51, 5.10, and 2.22, respectively, per formula unit and are consistent with divalent copper and cobalt ions.

Conclusions

In conclusion, our results suggest that hybrid molybdates can be crystallized in the presence of cobalt or copper pyrazole (or imidazole) complexes as templates. A pH value of about 6 is crucial for the formation of octamolybdate anion as well as for the stability of the metal complex. At this stage, predicting the exact nature of the metal complex and the type of octamolybdate anion (**A** or **B**) formed in a particular solid is difficult to rationalize. Reduction of the copper complex under hydrothermal conditions is apparent. However, it is almost impossible to determine beforehand whether a metal complex or organic moiety will act as a counter cation or derivatize the anion during crystallization. In this context, our proposal of hypothetical mechanisms for the occurrence of various hybrid crystals not only underlines the role of molecular recognition but also simplifies the crystal structure in terms of molecular bricks. The present work demonstrates how condensation of $[Mo_8O_{28}]$ cluster anions into 1D chains or 2D sheets is facilitated by hydrothermal conditions. We strongly believe that recognition of such molecular building blocks will allow us to rationalize the synthetic protocols to be employed for the design of such solids.

Experimental Section

Materials and Methods: All the starting materials were reagent grade and were used as purchased. The IR spectra were recorded with a Nicolet 5DX spectrophotometer with pressed KBr pellets. TG analyses were carried out with a Perkin–Elmer TGA7 and DTA7 system on well ground samples under flowing nitrogen with a heating rate of 10 °C min^{-1}. Room-temperature X-ray powder diffraction data were collected with a Bruker D8 Advance diffractometer using Ni-filtered Cu-K_α radiation. Data were collected with a step size of 0.02° and a count time of 2 s per step over the range $2° < 2\theta < 60°$. The susceptibility measurements as a function of temperature were performed with a SQUID magnetometer. Diamagnetic corrections were estimated from Pascal's constants.

Synthesis: A mixture of $(NH_4)_6Mo_7O_{24}{\cdot}4H_2O$ (0.7724 g, 0.625 mmol), $CuCl_2{\cdot}2H_2O$ (0.8524 g, 5 mmol), imidazole (imi; 0.5106 g, 7.5 mmol) and water (18 mL) was sealed in a Teflon-lined stainless-steel reactor and heated at various temperatures between 120 and 180 °C for three days. After the reaction, the system was slowly cooled down to room temperature. To rationalize the effect of the organic component as well as the metal ion, reactions with similar molar compositions were also carried out with pyrazole (pz) instead of imidazole and cobalt chloride instead of copper chloride. The reaction mixtures containing copper chloride and imidazole yielded two phases **1** (68% yield based on Mo) and **2** (71% yield based on Mo) at 150 and 120 °C, respectively, but the reaction between copper and pyrazole yielded **4** (84% yield based on Mo) at all temperatures between 120 and 180 °C. While the reaction mixture containing pyrazole and cobalt salt yielded **3** (87% yield based on Mo), the reaction between imidazole and cobalt resulted in a powder that could not be structurally characterized due to lack of suitable single crystals.

Crystallographic Studies: Single-crystal diffraction studies were carried out with a Bruker AXS SMART Apex CCD diffractometer

fitted with a Mo-K_α (0.71073 Å) radiation source at 28 °C for **1**–**4**. The software SADABS was used for absorption correction and SHELXTL for space group and structure determination and refinements.[48,49] The molybdenum atoms were located first and then remaining atoms were deduced from subsequent difference Fourier syntheses. The hydrogen atoms were located using geometrical constraints. All the atoms except H were refined anisotropically. The least-squares refinement cycles on F^2 were performed until the model converged. Experimental conditions and crystal data are provided in Tables 1 and 2, respectively.

Table 1. Experimental details.

Reactants/molar ratio	Phase	Color	Temperature (°C)	pH Initial[a]	Final[b]
$(NH_4)_6Mo_7O_{24}{\cdot}4H_2O$ + $CuCl_2{\cdot}2H_2O$ + imidazole + H_2O/18:12:1600	$[\{Cu(imi)_2\}_4(imi)_2Mo_8O_{26}]{\cdot}4H_2O$ (**1**)	brown	150	≈6	≈6
$(NH_4)_6Mo_7O_{24}{\cdot}4H_2O$ + $CuCl_2{\cdot}2H_2O$ + imidazole + H_2O/1:8:12:1600	$(Himi)_2[\{Cu(imi)_2\}_2Mo_8O_{27}]$ (**2**)	green	120	≈6	≈6
$(NH_4)_6Mo_7O_{24}{\cdot}4H_2O$ + $CoCl_2{\cdot}6H_2O$ + imidazole + H_2O/1:8:12:1600	Crystalline powder with no known phases. No suitable single crystals.	violet	120–180	≈6	≈6
$(NH_4)_6Mo_7O_{24}{\cdot}4H_2O$ + $CoCl_2{\cdot}6H_2O$ + pyrazole + H_2O/1:8:12:1600	$[\{Co(pz)_4\}_2(pz)_2Mo_8O_{26}]$ (**3**)	red	120–180	≈6	≈6
$(NH_4)_6Mo_7O_{24}{\cdot}4H_2O$ + $CuCl_2{\cdot}6H_2O$ + pyrazole + H_2O/1:8:12:1600	$[\{Cu(pz)_4\}_2Mo_8O_{26}]{\cdot}2H_2O$ (**4**)	blue	120–180	≈6	≈6

[a] pH of the initial reaction mixture before hydrothermal treatment. [b] pH of the filtrate after the crystals or solids have been separated.

Table 2. Crystallographic details.

	1	**2**	**3**	**4**
Crystal system	triclinic	triclinic	monoclinic	monoclinic
Space group	$P\bar{1}$	$P\bar{1}$	$P2_1/n$	$P2_1/n$
T [K]	300(2)	300(2)	300(2)	300(2)
a [Å]	9.6867(19)	9.429(3)	10.6172(16)	11.5849(8)
b [Å]	12.835(2)	9.875(4)	14.017(2)	18.4697(13)
c [Å]	12.981(3)	12.591(4)	19.030(3)	12.2645(9)
α [°]	67.868(3)	71.427(7)	90	90
β [°]	84.964(3)	81.358(7)	91.695(2)	94.18(0)
γ [°]	84.943(3)	72.474(7)	90	90
V [Å^3]	1486.6(5)	1057.7(6)	2831.0(7)	2617.25(30)
Z	1	1	2	2
Collected reflections	9087	6541	16800	15695
Unique reflections	5982	4285	6295	5994
Observed reflections	4629	2911	5204	4941
R_1 [$I > 2\sigma(I)$]	0.0395	0.0578	0.0350	0.0381
wR_2 (all)	0.0754	0.0984	0.0738	0.0837

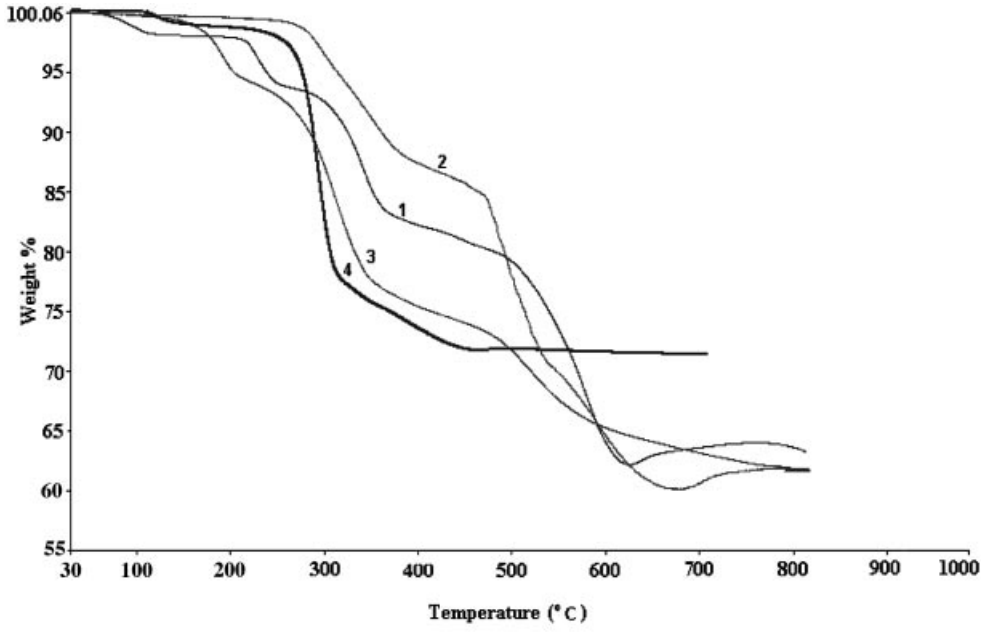

Figure 9. Thermogravimetric analysis for compounds **1**–**4**.

CCDC-284102 (for **1**), -284101 (for **2**), -284103 (for **3**) and -269635 (for **4**) contain the supplementary crystallographic data for this paper. These data can be obtained free of charge from The Cambridge Crystallographic Data Center via www.ccdc.cam.ac.uk/data_request/cif.

Vibrational Spectroscopy: In the IR spectrum of **1**, the peaks at 933, 890, 845, and 651 cm^{-1} are attributed to the $\nu(Mo\text{-}O_t)$ and $\nu(Mo\text{-}O_b)$ vibrational modes of the $[Mo_8O_{28}]^{8-}$ anion. Features at 3132, 2946, 1630, 1540, 1504, 1435, 1326, 1257, and 1181 cm^{-1} are characteristic absorptions of copper-coordinated imidazoles. The broad band at around 3371 cm^{-1} can be ascribed to the absorption of lattice water molecules. The IR spectra of **2** and **3** are similar to **1** expect that the peak at 3371 cm^{-1} is absent in the former, thus showing that there are no water molecules. The IR spectrum of **4** shows characteristic peaks at 945, 910, 849, 710, 666, and 551 cm^{-1} due to β-octamolybdate; the bands at 3132, 2946, 1630, 1540, 1504, 1435, 1326, 1257, and 1181 cm^{-1} are characteristic of copper-coordinated pyrazoles.

Thermal Stability of 1–4: The thermal dehydrations of **1**–**4** are quite different (Figure 9). All samples show a weight loss in multiple steps. For **1**, the loss of water molecules and free organic molecules and the decomposition of metal complexes occur in multiple steps. This observation clearly reflects the strength of hydrogen-bonding and other weak interactions noticed in the single crystal structure of the solids and was further confirmed by powder XRD and FTIR studies. The first two steps correspond to the loss of four water molecules and one organic group. The third and fourth steps correspond to degradation of the assembly. In **2**, the first step corresponds to the loss of two imidazole groups (≈ 200 °C) and the second step corresponds to the collapse of the structure with the loss of remaining organic groups. Complex **3** loses its organic groups in three steps. In the case of **4**, the loss of organic and water molecules was observed in the range 100–450 °C. In all cases the phase purity of the samples was further established by simulating powder X-ray diffraction patterns on the basis of the single-crystal structure data.

Supporting Information (see also the footnote on the first page of this article): Figures S1–S5 show additional figures for **1**–**4**, Figures S6–S9 show simulated and experimental powder X-ray diffraction patterns for **1**–**4**, and bond lengths and bond angles for **1**–**4** are given in Tables S10–S13.

Acknowledgments

K. P. thanks the Council of Scientific and Industrial Research, Government of India (CSIR) for a research fellowship and A. R. acknowledges the Department of Science and Technology, Government of India (DST), for financial support. We thank Dr. N. G. Ramesh for helpful discussion. A. R. also thanks the DST for funding a powder X-ray diffractometer under IRHPA and a Smart Apex CCD single-crystal X-ray diffractometer under FIST to the Department of Chemistry at IIT, Delhi. A. R. thanks Professor M. S. Whittingham for his support and encouragement during his sabbatical leave. S. E. L. acknowledges support from National Science Foundation and Materials Research Science and Engineering Centres (NSF MRSEC) DMR 0520471 and DMR 0603644.

[1] A. Müller, P. Kogerler, *Coord. Chem. Rev.* **1999**, *182*, 3–17.
[2] A. Müller, S. Roy, *Coord. Chem. Rev.* **2003**, *245*, 153–166.
[3] R. K. Grasselli, *Catal. Today* **1999**, *49*, 141–153.
[4] P. Kogerler, A. Müller, *J. Appl. Phys.* **2003**, *93*, 7101–7102.
[5] S. S. Kim, S. Ogura, H. Ikuta, Y. Uchimoto, M. Wakihara, *Solid State Ionics* **2002**, *146*, 249–256.
[6] Y. Song, P. Zhang, X. M. Ren, X. F. Shen, Y. Z. Li, X. Z. You, *J. Am. Chem. Soc.* **2005**, *127*, 3708–3709.
[7] J. B. Strong, G. P. A. Yap, R. Ostrander, L. M. L. Sands, A. L. Rheingold, R. Thouvenot, P. Gouzerh, E. A. Maatta, *J. Am. Chem. Soc.* **2000**, *122*, 639–649.
[8] T. Duraisamy, A. Ramanan, J. J. Vittal, *J. Mater. Chem.* **1999**, *9*, 763–767.
[9] B. Modec, J. V. Brencic, J. Zubieta, P. J. Hagrman, *Inorg. Chem. Commun.* **2001**, *4*, 537–540.
[10] P. Gili, P. A. L. Luis, A. Mederos, J. M. Arrieta, G. Germain, A. Castineiras, R. Carballo, *Inorg. Chim. Acta* **1996**, *295*, 106–114.
[11] Z. Kong, L. Weng, D. Tan, H. He, B. Zhang, J. Kong, B. Yue, *Inorg. Chem.* **2004**, *43*, 5676–5680.
[12] S. Upreti, A. Ramanan, *Inorg. Chim. Acta* **2005**, *358*, 1241–1246.
[13] B. Modec, J. V. Brencic, J. Zubieta, *Inorg. Chem. Commun.* **2003**, *6*, 506–512.
[14] N. Guillou, G. Ferey, *J. Solid State Chem.* **1997**, *132*, 224–227.
[15] C. D. Wu, C. Z. Lu, S. M. Chen, H. H. Zhang, J. S. Huang, *Polyhedron* **2003**, *22*, 3091–3095.
[16] C. Z. Lu, C. D. Wu, H. H. Zhang, J. S. Huang, *Chem. Mater.* **2002**, *14*, 2649–2655.
[17] D. Hagrman, C. Sangregorio, C. J. O'Connor, J. Zubieta, *J. Chem. Soc., Dalton Trans.* **1998**, 3707–3710.
[18] S. Upreti, A. Ramanan, *Cryst. Growth Des.* **2005**, *5*, 1837–1843; S. Upreti, A. Ramanan, *Cryst. Growth Des.* **2006**, *6*, 2066–2071.
[19] P. J. Hagrman, D. Hagrman, J. Zubieta, *Angew. Chem. Int. Ed.* **1999**, *38*, 2638–2684.
[20] K. Pavani, A. Ramanan, *Eur. J. Inorg. Chem.* **2005**, 3080 –3087.
[21] S. Randy Jr., R. S. Rarig, J. Zubieta, *J. Solid State Chem.* **2002**, *167*, 370–375.
[22] D. G. Allis, R. S. Rarig, E. Burkholder, J. Zubieta, *J. Mol. Struct.* **2004**, *688*, 11–31.
[23] S. M. Chen, C. Z. Lu, Y. Q. Yu, Q. Z. Zhang, X. He, *Inorg. Chem. Commun.* **2004**, *7*, 1041–1044.
[24] W. Yang, C. Lu, H. Zhuang, *J. Chem. Soc., Dalton Trans.* **2002**, 2879–2884.
[25] C. Z. Lu, C. D. Wu, H. H. Zhuang, J. S. Huang, *Chem. Mater.* **2002**, *14*, 2649–2655.
[26] R. S. Rarig, J. Zubieta, *Polyhedron* **2003**, *22*, 177–188.
[27] M. Isobe, F. Marumo, T. Yamase, T. Ikawa, *Acta Crystallogr., Sect. B* **1978**, *34*, 2728–2731.
[28] W. Wang, L. Xu, Y. Wei, F. Lia, G. Gao, E. Wang, *J. Solid State Chem.* **2005**, *178*, 608–612.
[29] D. Attanasio, M. Bonamico, V. Fares, L. Suber, *J. Chem. Soc., Dalton Trans.* **1992**, 2523–2528.
[30] B. M. Gatehouse, P. Leverette, *J. Chem. Soc. A* **1971**, 2107–2112.
[31] R. Benchrifa, M. Leblanc, R. de Pape, *Eur. J. Solid State Inorg. Chem.* **1989**, *26*, 593–601.
[32] J. Kang, Q. Z. Zhang, C. D. Wu, W. B. Yang, X. P. Zhan, Y. Q. Yu, C. Z. Lu, *Chin. J. Struct. Chem.* **2003**, *22*, 190–194.
[33] A. Ramanan, M. S. Whittingham, *Cryst. Growth Des.* **2006**, *6*, 2419–2421.
[34] K. Pavani, A. Ramanan, M. S. Whittingham, *J. Mol. Struct.* **2006**, *796*, 179–186.
[35] X. You, J. Chen, Z. Xu, J. Huang, *Acta Crystallogr., Sect. C* **1989**, *45*, 413–415.
[36] R. D. Adams, W. G. Klemperer, R. S. Lui, *J. Chem. Soc., Chem. Commun.* **1979**, 256–257.
[37] C. D. Wu, C. Z. Lu, H. H. Zuang, J. S. Huang, *Inorg. Chem.* **2002**, *41*, 5636–5637.
[38] J. Luo, M. Hong, R. Wang, Q. Shi, R. Cao, J. Weng, R. Sun, H. Zhang, *Inorg. Chem. Commun.* **2003**, *6*, 702–705.
[39] X. B. Cui, K. Lu, Y. Fan, J. O. Xu, L. Yeb, Y. H. Sun, Y. Li, H. H. Yu, Z. H. Yi, *J. Mol. Struct.* **2005**, *743*, 151–155.
[40] C. D. Wu, C. Z. Lu, W. B. Yang, S. F. Lu, H. H. Zhaung, J. Huang, *J. Cluster. Sci.* **2002**, *13*, 55–62.

[41] I. Boeschen, B. Buss, B. Krebs, *Acta Crystallogr., Sect. B* **1974**, *30*, 48–56.
[42] W. T. A. Harrison, L. L. Dussack, A. J. Jacobson, *Acta Crystallogr., Sect. C* **1996**, *52*, 1075–1077.
[43] T. Yamase, T. Ozeki, I. Kawashima, *Acta Crystallogr. Sect. C* **1995**, *51*, 545–547.
[44] T. Yamase, H. Naruke, *J. Chem. Soc., Dalton Trans.* **1991**, 285–292.
[45] D. Hagrman, P. J. Hagrman, J. Zubieta, *Comments Inorg. Chem.* **1999**, *21*, 225–261.
[46] C. D. Wu, C. Z. Lu, H. Zhuang, J. Huang, *Inorg. Chem.* **2002**, *41*, 5636–5637.
[47] J. R. D. DeBord, R. C. Haushalter, L. M. Meyer, D. J. Rose, P. J. Zapf, J. Zubieta, *Inorg. Chim. Acta* **1997**, *256*, 165–168.
[48] G. M. Sheldrick, *Acta Crystallogr., Sect. A* **1990**, *46*, 467–473.
[49] G. M. Sheldrick, SHELXTL-NT2000, version 6.12, reference manual, University of Göttingen, Germany.

Received: September 6, 2006
Published Online: December 7, 2006

